

Stability and flying qualities analysis of flexible aircraft by coupling the Vortex Lattice method and the discontinuous Galerkin method

Fernando Montano and Ivano Benedetti* and Vincenzo Gulizzi*[†]*

**Department of Engineering, Università degli Studi di Palermo
Viale delle Scienze, Building 8, 90128, Palermo, Italy*

fernando.montano@unipa.it · ivano.benedetti@unipa.it · vincenzo.gulizzi@unipa.it

[†]Corresponding author

Abstract

This contribution presents a novel computational approach to aeroelasticity based on the combined use of the Vortex Lattice Method and the discontinuous Galerkin method. The proposed procedure is the first step towards the development of a tool for the optimization, control and morphing of flexible aircraft featuring improved stability and flying performances. Preliminary numerical results are presented for the static aeroelastic behavior of wings with flat-plate and thin-walled NACA profiles. The obtained results show the accuracy and the potential of the proposed approach.

1. Introduction

Some aeronautical applications, e.g. high altitude experimental aircraft, MALE and HALE UAVs, favor the use of high aspect ratio wings, by virtue of their higher lift-to-drag ratio that contributes to reducing fuel consumption. However, high aspect ratios also imply higher structural flexibility so that, in the evaluation of the aircraft stability and flying qualities, it is not possible to decouple the flight dynamics from the elastic response.^{1,17,21}

Aeroelasticity is a complex problem falling in the area of fluid structure interaction (FSI), which requires the coupled solution of solid and fluid mechanics simulations. Aeroelastic analysis may be tackled by the combination of Computational Fluid Dynamics (CFD) with Finite Element Methods (FEMs), see e.g. Refs.^{7,8} Despite their accuracy and capabilities, such procedures require high computational costs in terms of data preparation, storage memory and solution time, which are not always affordable, especially during the conceptual design phase. To overcome such limitations, other lower-order aerodynamic computational techniques, such as the Vortex Lattice Method (VLM), have been developed. Under some assumptions and in well defined flight regimes, VLM provides accurate enough results in less time with respect to full-field CFD. It is known that, at low angles of attack, CFD and VLM deliver similar results in terms of trim conditions with small difference in pressure distribution.²⁰

For such reasons, VLM is widely used today for conceptual and trade-off studies, when several alternative configurations need to be quickly evaluated, before selecting the most promising alternatives. VLM has been employed to investigate the non-planar aerodynamics of flexible wings with large deformation, coupled with FEM for structural nonlinear analysis,²² or for aeroelastic loads evaluation on wings then analyzed with extended beam models.³ VLM has also been extended to compressible flows for non-linear aeroelastic analysis.¹⁸ VLM is also widely employed as the reference aerodynamic tool in several studies investigating the effects of aeroelastic deformations on flight dynamics performance. Results from the Unsteady Vortex Lattice Method (UVLM) could be directly applicable in the identification of appropriate modeling strategies in nonlinear flexible aircraft flight dynamics simulations.¹⁹ The Doublet Lattice Method (DLM) has been used in a coupled lateral-directional flight dynamic and aeroelastic study of a Prandtl-plane configuration.⁶ Aerodynamic forces obtained by VLM have been used to validate results in a new framework for coupled non-linear aeroelasticity and flight dynamics of highly flexible aircrafts.²³

This work proposes the coupling of VLM with discontinuous Galerkin (DG) methods for solving the static aeroelastic problem of wing structures. With respect to other numerical techniques for solid mechanics, DG methods naturally offers high-order accuracy with generic mesh elements and ease of parallelization.

The paper is organized as follows: Sec.(2) describes the considered aeroelastic problem introducing the employed aerodynamic model, the structural model and their coupling; Sec.(3) presents a few numerical results obtained by the present approach; and Sec.(4) draws the conclusions and outlines avenues of future research.

2. Problem statement

2.1 Aerodynamic model

The aerodynamic model employed in this study uses the VLM, a low- to medium-fidelity tool that allows evaluating the aerodynamics of wings for high-Reynolds, low-speed attached flows. The underlying hypotheses and the development of the numerical methods based on the VLM are well known and are not reported here. Nevertheless, it is worth noting that the VLM implementation considered in this study allows modeling generally curved lifting surfaces. The reader interested in the detail of the method is referred to classical aerodynamics books.¹⁶

2.2 Structural model

The structural behavior of the wing is modeled by a recently developed formulation for beam structures,¹² that extends previous studies on composite plates^{13,14} and shells.⁹⁻¹¹ The formulation is based on the discontinuous Galerkin methods for elliptic PDEs² and provides high-accurate resolution of the displacement fields throughout both the wing cross section and the wing length.

We consider a wing that may be represented as a beam with length L and cross-section Ω . We introduce a three-dimensional reference system $Ox_1x_2x_3$ located at the root of the wing and defined such that length of the wing is spanned by the coordinate x_2 while its cross-section is spanned by x_1 and x_3 .

The mechanical behavior of the wing is represented by the vector $\mathbf{u} = (u_1, u_2, u_3)^\top$ of the displacement components and the vectors $\boldsymbol{\sigma} = (\sigma_{11}, \sigma_{22}, \sigma_{33}, \sigma_{23}, \sigma_{13}, \sigma_{12})^\top$ and $\boldsymbol{\gamma} = (\gamma_{11}, \gamma_{22}, \gamma_{33}, \gamma_{23}, \gamma_{13}, \gamma_{12})^\top$, which collect the components of the strain and stress tensors, respectively, using Voigt notation. We also introduce the vector $\bar{\mathbf{t}} = (\bar{t}_1, \bar{t}_2, \bar{t}_3)^\top$ of the prescribed surface traction components and the vector $\bar{\mathbf{b}} = (\bar{b}_1, \bar{b}_2, \bar{b}_3)^\top$ of the known volume forces. Upon assuming that the wing behaves as a linear elastic solid undergoing small deformations, the strain-displacement relation and the stress-strain relation may be written as

$$\boldsymbol{\gamma} = \mathbf{I}_k \frac{\partial \mathbf{u}}{\partial x_k} \quad \text{and} \quad \boldsymbol{\sigma} = \mathbf{C} \boldsymbol{\gamma}, \quad (1)$$

respectively, where \mathbf{I}_k , with $k = 1, 2, 3$, are 6×3 matrices containing ones and zeros only,¹³ and \mathbf{C} is the 6×6 matrix containing the elastic coefficients. In Eq.(1) and in the remainder of this paper, Latin subscripts take values in $\{1, 2, 3\}$, Greek subscripts take values in $\{1, 3\}$ and summation is implied when subscripts are repeated.

In the context of high-order beam theories,⁴ the displacement field \mathbf{u} is expressed as the sum of products of known functions of the cross-section coordinates x_1 and x_3 and unknown functions of the lengthwise coordinate x_2 . Such an expansion may be conveniently expressed using the following matrix expression¹²⁻¹⁴

$$\mathbf{u} = \mathbf{Z}(x_1, x_3) \mathbf{U}(x_2), \quad (2)$$

where $\mathbf{U}(x_2)$ is a N_u -dimensional vector containing the unknown functions of x_2 , which are also referred to as generalized displacements, and $\mathbf{Z}(x_1, x_3)$ is a $3 \times N_u$ matrix containing the known cross-section functions of x_1 and x_3 . Here, N_u denotes the order of expansion of the selected high-order beam theory and is defined as $N_u \equiv (N_{u_1} + N_{u_2} + N_{u_3} + 3)$, where N_{u_k} is the order of expansion of the k -th displacement component.

The governing equations associated with high-order beam theories are derived from the Principle of Virtual Displacement (PVD) of three-dimensional elasticity. In particular, using Eq.(2) into the PVD, integrating the mechanical variables across the wing cross-section, and performing integration by parts, it is possible to show¹² that wings modeled by high-order beam theories are governed by the following set of differential equations

$$-\frac{d}{dx_2} \left(\mathbf{Q} \frac{d\mathbf{U}}{dx_2} + \mathbf{R} \mathbf{U} \right) + \mathbf{R}^\top \frac{d\mathbf{U}}{dx_2} + \mathbf{S} \mathbf{U} = \bar{\mathbf{B}} \quad \text{for } x_2 \in \mathcal{D}, \quad (3)$$

where $\mathcal{D} \equiv [0, L]$ denotes the modeling domain of the beam, the terms \mathbf{Q} , \mathbf{R} and \mathbf{R} are $N_u \times N_u$ generalized stiffness matrices defined as follows

$$\mathbf{Q} \equiv \int_{\Omega} \mathbf{Z}^\top \mathbf{c}_{22} \mathbf{Z} \, d\Omega, \quad \mathbf{R} \equiv \int_{\Omega} \mathbf{Z}^\top \mathbf{c}_{2\alpha} \frac{\partial \mathbf{Z}}{\partial x_\alpha} \, d\Omega, \quad \text{and} \quad \mathbf{S} \equiv \int_{\Omega} \frac{\partial \mathbf{Z}^\top}{\partial x_\alpha} \mathbf{c}_{\alpha\beta} \frac{\partial \mathbf{Z}}{\partial x_\beta} \, d\Omega, \quad (4)$$

with $c_{kl} \equiv \mathbf{I}_k^\top \mathbf{C} \mathbf{I}_l$, and $\bar{\mathbf{B}}$ is the vector of generalized domain loads defined as

$$\bar{\mathbf{B}} \equiv \int_{\Omega} \mathbf{Z}^\top \bar{\mathbf{b}} \, d\Omega + \int_{\partial\Omega} \mathbf{Z}^\top \bar{\mathbf{t}} \, d\partial\Omega. \quad (5)$$

Eventually, we assume that the wing is subjected to fixed boundary conditions at its root section, i.e. $\mathbf{U} = 0$ at $x_2 = 0$, and traction-free boundary conditions at its tip section.

2.3 Discontinuous Galerkin formulation

The discontinuous Galerkin formulation for the structural model presented in Sec.(2.2) is derived following the Interior Penalty DG approach previously employed for composite plates^{13,14} and shells⁹⁻¹¹ and applied here to the one-dimensional beam problems. In particular, the domain \mathcal{D} is divided into N_e non-overlapping elements, i.e. $\mathcal{D} \approx \mathcal{D}^h \equiv \bigcup_{e=1}^{N_e} \mathcal{D}^e$, where \mathcal{D}^e is a generic e -th element. The space \mathcal{V}^{hp} of discontinuous basis functions is introduced as follows

$$\mathcal{V}^{hp} \equiv \{v : \mathcal{D}^h \rightarrow \mathbb{R} \mid v(x_2 \in \mathcal{D}^e) \in \mathcal{P}^p(\mathcal{D}^e) \forall e = 1, \dots, N_e\}, \quad (6)$$

where $\mathcal{P}^p(\mathcal{D}^e)$ is the space of polynomials up to degree p defined over the element \mathcal{D}^e . Then, it is possible to show that the DG-based discrete solution \mathbf{U}^h of Eq.(3) with the associated boundary conditions must satisfy

$$B_{\text{IP}}(\mathbf{V}, \mathbf{U}^h) = L_{\text{IP}}(\mathbf{V}, \bar{\mathbf{B}}) \quad (7)$$

for any $\mathbf{V} \in (\mathcal{V}^{hp})^{N_u}$, where

$$\begin{aligned} B_{\text{IP}}(\mathbf{V}, \mathbf{U}^h) \equiv & \int_{\mathcal{D}^h} \left[\frac{d\mathbf{V}^\top}{dx_2} \left(\mathbf{Q} \frac{d\mathbf{U}^h}{dx_2} + \mathbf{R} \mathbf{U}^h \right) + \mathbf{V}^\top \left(\mathbf{R}^\top \frac{d\mathbf{U}^h}{dx_2} + \mathbf{S} \mathbf{U}^h \right) \right] dx_2 + \\ & - \sum_{x_2 \in \mathcal{I}^h} \left(\llbracket \mathbf{V} \rrbracket^\top \left\{ \mathbf{Q} \frac{d\mathbf{U}^h}{dx_2} + \mathbf{R} \mathbf{U}^h \right\} + \left\{ \frac{d\mathbf{V}^\top}{dx_2} \mathbf{Q} + \mathbf{V}^\top \mathbf{R}^\top \right\} \llbracket \mathbf{U}^h \rrbracket \right) + \sum_{x_2 \in \mathcal{I}^h} \mu \llbracket \mathbf{V} \rrbracket^\top \llbracket \mathbf{U}^h \rrbracket \\ & - \left(\gamma_{x_2} \mathbf{V}^\top \left(\mathbf{Q} \frac{d\mathbf{U}}{dx_2} + \mathbf{R} \mathbf{U} \right) + \left(\frac{d\mathbf{V}^\top}{dx_2} \mathbf{Q} + \mathbf{V}^\top \mathbf{R}^\top \right) \mathbf{U}^h \right)_{x_2=0} + \left(\mu \mathbf{V}^\top \mathbf{U}^h \right)_{x_2=0} \end{aligned} \quad (8)$$

and

$$L_{\text{IP}}(\mathbf{V}, \bar{\mathbf{B}}) \equiv \int_{\mathcal{D}^h} \mathbf{V}^\top \bar{\mathbf{B}} dx_2. \quad (9)$$

In Eqs.(8) and (9), the terms $\{\bullet\}$ and $\llbracket \bullet \rrbracket$ denotes the so-called average and jump operators, defined as

$$\{\bullet\} \equiv \frac{1}{2}(\bullet^e + \bullet^{e+1}) \quad \text{and} \quad \llbracket \bullet \rrbracket \equiv \bullet^e - \bullet^{e+1}, \quad (10)$$

the term $\int_{\mathcal{D}^h} \bullet dx_2 \equiv \sum_e \int_{\mathcal{D}^e} \bullet dx_2$ denotes the so-called broken integral, \mathcal{I}^h is the set of inter-element interfaces, and ν_{x_2} is the element's outward unit normal. Note that, being the beam model one-dimensional, $\nu_{x_2}^e = -1$ and $\nu_{x_2}^e = +1$ for $x_2 = y_-^e$ and $x_2 = y_+^e$, respectively, where y_-^e and y_+^e are the two end points of the e -th element.

2.4 Aeroelastic coupling

The coupling between the VLM introduced in Sec.(2.1) and the DG formulation for beam structures introduced in Sec.(2.3) is discussed in this section. Two models are valid for steady-state aerodynamics and static elasticity; therefore, it is worth noting that the aeroelastic coupling considered here is to be intended as static aeroelastic coupling.

According to the VLM discretization strategy,¹⁶ the wing is replaced by N_v vortices of unknown strength; then, upon enforcing the non-penetrability condition of the velocity field through the lifting surface, the VLM leads to the following system of algebraic equations

$$\mathbf{A} \mathbf{\Gamma} = \mathbf{B}, \quad (11)$$

where $\mathbf{\Gamma}$ is a N_v -dimensional vector collecting the unknown strengths of the vortices, \mathbf{A} is $N_v \times N_v$ matrix of the aerodynamic influence coefficients and \mathbf{B} is the N_v -dimensional right-hand side vector that is function of the free-stream velocity V_∞ .

The DG method also leads to a linear system of equations. In particular, upon expressing \mathbf{U}^h as the product of known basis functions and unknown coefficients for each mesh element, and letting \mathbf{V} range over the basis functions, it is possible to show¹⁵ that Eq.(7) leads to an algebraic system of the form

$$\mathbf{K} \mathbf{X} = \mathbf{F}_S + \mathbf{F}_A, \quad (12)$$

where: \mathbf{X} is a $(N_p N_e)$ -dimensional vector collecting the unknown DG coefficients, with N_p being the number of unknown coefficients (or basis functions) per each element; \mathbf{K} is the stiffness matrix of the wing structure; \mathbf{F}_S is the

DG METHODS FOR AEROELASTIC FLEXIBLE AIRCRAFT

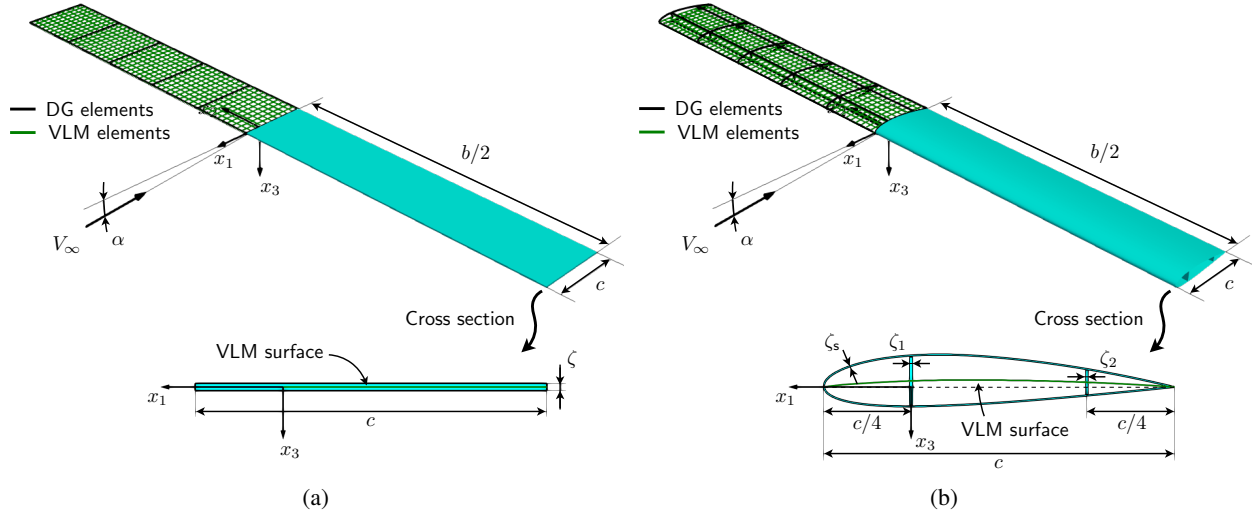


Figure 1: (a) Wing with a flat-plate cross-section. (b) Wing with a thin-walled airfoil-shaped cross-section

right-hand side vector stemming from the structural loads, such as weight or concentrated forces; and \mathbf{F}_A is the right-hand side vector stemming from the aerodynamic loads obtained by the VLM.

The coupling between Eq.(11) and Eq.(12) is two-fold. On the one hand, \mathbf{F}_A directly depends on the vortices strengths, i.e. $\mathbf{F}_A = \mathbf{F}_A(\boldsymbol{\Gamma})$. On the other hand, the location and the tangent plane at the VLM control points, where the non-penetrability condition is enforced, depend on the deformation of the structure; this means that the matrices \mathbf{A} and \mathbf{B} in Eq.(11) depend on \mathbf{X} . Although such a coupling is in general non-linear, it is possible to linearize Eqs.(11) and (12) as

$$\mathbf{A}_0 \boldsymbol{\Gamma} = \mathbf{B}_0 + \frac{\partial \mathbf{B}}{\partial \mathbf{X}} \mathbf{X} \quad (13)$$

and

$$\mathbf{K} \mathbf{X} = \mathbf{F}_S + \frac{\partial \mathbf{F}_A}{\partial \boldsymbol{\Gamma}} \boldsymbol{\Gamma}, \quad (14)$$

respectively, where the matrices \mathbf{A}_0 and \mathbf{B}_0 are obtained by the VLM discretization for the wing in the undeformed configuration. Combining Eqs.(13) and (14) leads to the static aeroelastic problem

$$\mathbf{K}_{AE} \mathbf{X} = \mathbf{F}_{AE}, \quad (15)$$

where

$$\mathbf{K}_{AE} \equiv \mathbf{K}_S - \frac{\partial \mathbf{F}_A}{\partial \boldsymbol{\Gamma}} \mathbf{A}_0^{-1} \frac{\partial \mathbf{B}}{\partial \mathbf{X}} \quad \text{and} \quad \mathbf{F}_{AE} \equiv \mathbf{F}_S + \mathbf{A}_0^{-1} \mathbf{B}_0. \quad (16)$$

Eventually, upon noting that \mathbf{B} and \mathbf{F}_A may be written as $\mathbf{B} = V_\infty \widehat{\mathbf{B}}$ and $\mathbf{F}_A = \rho_\infty V_\infty \widehat{\mathbf{F}}_A$, where $\widehat{\mathbf{B}}$ and $\widehat{\mathbf{F}}_A$ are computed assuming unitary free-stream velocity V_∞ and free-stream density ρ_∞ , Eq.(16) allows computing the divergence speed V_D for the considered wing configuration by solving the following eigenvalue problem

$$\left(\mathbf{K}_S - \rho_\infty V_D^2 \frac{\partial \widehat{\mathbf{F}}_A}{\partial \boldsymbol{\Gamma}} \mathbf{A}_0^{-1} \frac{\partial \widehat{\mathbf{B}}}{\partial \mathbf{X}} \right) \mathbf{X} = \mathbf{0}. \quad (17)$$

3. Results

In this section, the tool developed in the preceding section is employed to solve the aeroelastic problem for two wing structures. We consider a wing with a flat-plate cross-section and a wing with a airfoil-shaped thin-walled cross section as shown in Fig.(1a) and Fig.(1b), respectively. Both structures are made of isotropic aluminium with Young's modulus $E = 69$ GPa and Poisson's ratio $\nu = 0.33$.

The first set of results investigates the effect of the order p of the basis functions of the DG method on the convergence performance of the proposed formulation. We consider the wing with the flat-plate cross-section having $c = 1$ m, $b/2 = 5$ m and $\zeta = 0.02$ m, see Fig.(1a). The wing is modeled using a third-order beam theory (BT) and is subjected to a free-stream velocity $V_\infty = 30$ m/s and an angle of attack $\alpha = 1^\circ$. A 10×50 lattice is employed as the VLM mesh. The maximum deflection and the twist of the wing tip are reported in Fig.(2) as a function of the basis

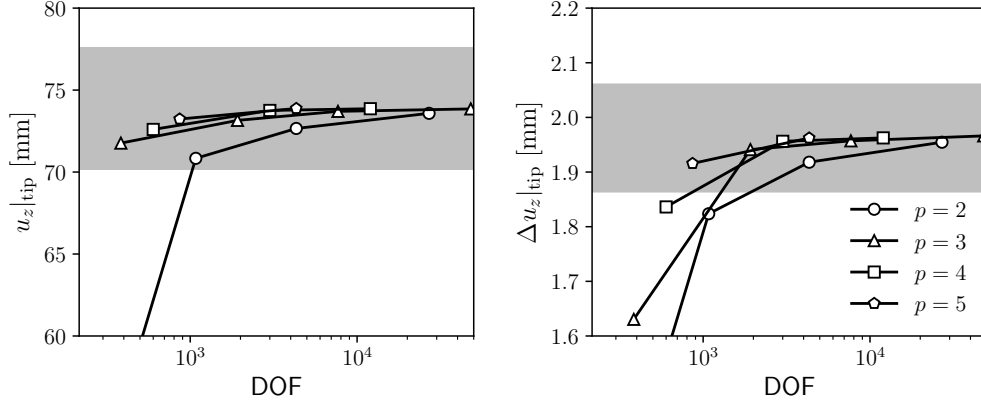


Figure 2: Convergence results for (left) the wing tip maximum deflection $u_z|_{\text{tip}}$ and (right) the wing tip twist $\Delta u_z|_{\text{tip}}$.

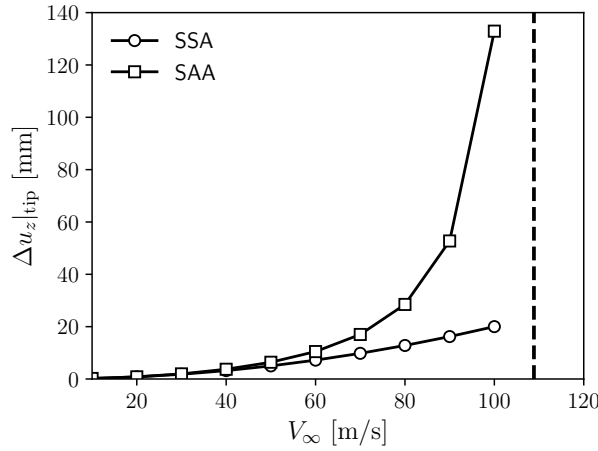


Figure 3: Wing tip twist as a function of the free-stream velocity approaching the divergence speed (the dashed line).

functions order p and the overall number of degrees of freedom of the discrete system. In figure, data points with the same marker are obtained by changing the number of mesh elements of the structural mesh, whilst the gray area denotes the region with less than 5% deviation from the result obtained with largest number of degrees of freedom. From the plots, it is clear that higher-order approximations achieve faster convergence to the solution and require fewer degrees of freedom than the corresponding lower order schemes.

In the second of test, we investigate the effect of the free-stream velocity on the twist of the wing tip upon considering the static aeroelastic analysis (SAA) given in Eq.(15) as opposed to considering a static structural analysis (SSA) only, whereby the aerodynamic loads are transferred to the structure without the aeroelastic coupling. We consider the same wing as the previous set of test modeled using a 5-element structural mesh with basis functions order $p = 5$, and keep all other parameters unchanged. The obtained results are reported in the plot of Fig.(3), which shows the expected behavior of the aeroelastic response as the velocity approaches the divergence speed computed using Eq.(17).

The third set of tests shows the effect of the wing span b on the wing tip maximum deflection for the SAA and the SSA cases. Unlike the previous cases, the wing has a thickness $\zeta = 0.1$ m, is subjected to a free-stream flow at $V_\infty = 70$ m/s. All other parameters are kept unchanged. The computed results are reported in Tab.(1) for different wing span values and beam theories; the comparison with the results available in the literature confirms the accuracy of the present formulation.

In the fourth set of tests, we consider the wing with the airfoil-shaped thin-walled cross-section. With reference to Fig.(1b), the geometrical properties of the wing are $b/2 = 5$ m, $\zeta_s/c = 0.006$, $\zeta_1/c = 0.015$, $\zeta_2/c = 0.0105$. The wing is subjected to the free-stream conditions $V_\infty = 50$ m/s and $\alpha = 3^\circ$, and is modeled via a fourth-order beam theory and a 5-element structural mesh with $p = 5$. In this case, we investigate the effect of using a flat VLM formulation, where the vortices lattice is obtained by discretizing the chords surface of the wing, as opposed to using a curved VLM formulation, where the vortices lattice is obtained by discretizing the mean-thickness surface of the wing. It is worth

Table 1: Wing tip maximum deflection in mm as a function of the wing span b and different structural theories.

$b/2$ [m]		BT ₁		BT ₂		BT ₃		BT ₄		NASTRAN
		Ref. ⁵	Present							
5	SSA	2.9928	2.9499	2.8620	2.9324	2.9192	2.9340	2.9325	2.9361	-
	SAA	2.9933	2.9622	2.8731	2.9445	2.9307	2.9462	2.9443	2.9483	2.9505
10	SSA	56.366	55.671	54.631	55.426	55.358	55.438	55.478	55.470	-
	SAA	56.402	56.845	55.717	56.585	56.465	56.605	56.611	56.637	56.723
20	SSA	1000.3	990.83	981.43	987.73	988.76	987.87	989.72	988.21	-
	SAA	1003.0	1091.8	1075.8	1087.6	1084.1	1088.4	1087.3	1088.8	1092.8

Table 2: Wing tip maximum deflection in mm obtained using a flat VLM surface versus a curved VLM surface.

	Ref. ⁵	Flat VLM	Curved VLM
SSA	8.6854	8.8967	9.2117
SAA	8.8377	8.9159	9.2018

stressing that the angle of attack is to be considered with respect to the zero-lift direction, which, for the curved VLM case, has been evaluated as $\alpha_0 = -2.1396^\circ$. The obtained results are reported in Tab.(2) for the SAA and the SSA cases, and recover the results obtained in the literature by Carrera et al.,⁵ who also employed a flat VLM discretization.

4. Conclusions

A novel numerical approach to static aeroelasticity has been presented in this research study. The proposed formulation uses the VLM to solve the aerodynamic problem and high-order DG-based beam theories to solve the structural problem of wing structures. The coupling between the two methods has been discussed and numerically tested. The obtained results have confirmed the accuracy and shown the potential of the formulation.

The presented methodology serves as a first step towards the development of a fast tool for estimating the flight dynamics performances of highly flexible aircraft during preliminary design stages. Future studies will be devoted to the application of the method to unsteady aeroelasticity, to the study of the wing-tail coupling and to the analysis of different morphing wing configurations for improved flight performances.

5. Acknowledgments

FM and IB acknowledge the support of the European Union through the FESR o FSE, PON Ricerca e Innovazione 2014-2020 - DM 1062/2021 co-funding scheme. FM and VG acknowledge the support of the Department of Engineering of the University of Palermo through the grant Premio Gruppi di Ricerca 2022. IB and VG also acknowledge support from the EU – NextGeneration EU – MUR D.M. 737/2021 – research project ClearWay EUROSTART (PRJ-0993).

References

- [1] F. Afonso, J. Vale, É. Oliveira, F. Lau, and A. Suleman. A review on non-linear aeroelasticity of high aspect-ratio wings. *Progress in Aerospace Sciences*, 89:40–57, 2017.
- [2] D.N. Arnold, F. Brezzi, B. Cockburn, and L.D. Marini. Unified analysis of discontinuous Galerkin methods for elliptic problems. *SIAM journal on numerical analysis*, 39(5):1749–1779, 2002.
- [3] K. Bramsiepe, T. Klimmek, W.-R. Krüger, and L. Tichy. Aeroelastic method to investigate nonlinear elastic wing structures. *CEAS Aeronautical Journal*, 13(4):939–949, 2022.
- [4] E. Carrera and M. Petrolo. On the effectiveness of higher-order terms in refined beam theories. *Journal of Applied Mechanics*, 78(2):021013, 2011.
- [5] E. Carrera, A. Varello, and L. Demasi. A refined structural model for static aeroelastic response and divergence of metallic and composite wings. *CEAS Aeronautical Journal*, 4(2):175–189, 2013.

- [6] R. Cavallaro and R. Bombardieri. Studies on lateral-directional coupled flight dynamics and aeroelasticity of a PrandtlPlane. In *AIAA Scitech 2019 Forum*, page 1118, 2019.
- [7] M. Grifò, A. Da Ronch, and I. Benedetti. A computational aeroelastic framework based on high-order structural models and high-fidelity aerodynamics. *Aerospace Science and Technology*, 132:108069, 2023.
- [8] M. Grifò, V. Gulizzi, A. Milazzo, A. Da Ronch, and I. Benedetti. High-fidelity aeroelastic transonic analysis using higher-order structural models. *Composite Structures*, page 117315, 2023.
- [9] G. Guarino, V. Gulizzi, and A. Milazzo. High-fidelity analysis of multilayered shells with cut-outs via the discontinuous Galerkin method. *Composite Structures*, 276:114499, 2021.
- [10] G. Guarino, V. Gulizzi, and A. Milazzo. Accurate multilayered shell buckling analysis via the implicit-mesh discontinuous Galerkin method. *AIAA Journal*, 60(12):6854–6868, 2022.
- [11] G. Guarino, A. Milazzo, and V. Gulizzi. Equivalent-single-layer discontinuous Galerkin methods for static analysis of multilayered shells. *Applied Mathematical Modelling*, 98:701–721, 2021.
- [12] V. Gulizzi, I. Benedetti, and A. Milazzo. High-order accurate beam models based on discontinuous Galerkin methods. *Submitted*.
- [13] V. Gulizzi, I. Benedetti, and A. Milazzo. A high-resolution layer-wise discontinuous Galerkin formulation for multilayered composite plates. *Composite Structures*, 242:112137, 2020.
- [14] V. Gulizzi, I. Benedetti, and A. Milazzo. An implicit mesh discontinuous Galerkin formulation for higher-order plate theories. *Mechanics of Advanced Materials and Structures*, 27(17):1494–1508, 2020.
- [15] V. Gulizzi, I. Benedetti, and A. Milazzo. Discontinuous Galerkin methods for solids and structures. In M.H.F. Aliabadi and W.O. Soboyejo, editors, *Comprehensive Structural Integrity (Second Edition)*, pages 348–377. Elsevier, Oxford, second edition, 2023.
- [16] J. Katz and A. Plotkin. *Low-speed aerodynamics*, volume 13. Cambridge university press, 2001.
- [17] J. Murua, R. Palacios, and J.M.R. Graham. Applications of the unsteady vortex-lattice method in aircraft aeroelasticity and flight dynamics. *Progress in Aerospace Sciences*, 55:46–72, 2012.
- [18] M. Parenteau and E. Laurendeau. A transonic, viscous nonlinear frequency domain Vortex Lattice Method for aeroelastic analyses. *Journal of Fluids and Structures*, 107:103406, 2021.
- [19] R. J. Simpson and R. Palacios. Numerical aspects of nonlinear flexible aircraft flight dynamics modeling. In *54th AIAA/ASME/ASCE/AHS/ASC Structures, Structural Dynamics, and Materials Conference*, page 1634, 2013.
- [20] A. Voß. Comparison between VLM and CFD maneuver loads calculation at the example of a flying wing configuration. *Journal of Aeroelasticity and Structural Dynamics*, pages 19–37, 2019.
- [21] J.R. Wright and J.E. Cooper. *Introduction to aircraft aeroelasticity and loads*, volume 20. John Wiley & Sons, 2008.
- [22] C. Xie, L. Wang, C. Yang, and Y. Liu. Static aeroelastic analysis of very flexible wings based on non-planar vortex lattice method. *Chinese Journal of Aeronautics*, 26(3):514–521, 2013.
- [23] C. Zhang, Z. Zhou, X. Zhu, and L. Qiao. A Comprehensive Framework for Coupled Nonlinear Aeroelasticity and Flight Dynamics of Highly Flexible Aircrafts. *Applied Sciences*, 10(3), 2020.